

Intersubband transitions in InAs/AlSb quantum wells studied by resonant Raman scattering

J. Wagner, J. Schmitz, F. Fuchs, J. D. Ralston, and P. Koidl

Fraunhofer-Institut für Angewandte Festkörperphysik, Tullastrasse 72, D-79108 Freiburg, Federal Republic of Germany

D. Richards

Cavendish Laboratory, Madingley Road, Cambridge CB3 0HE, United Kingdom

(Received 7 December 1994)

We have used resonant Raman scattering to study intersubband transitions in InAs/AlSb quantum wells. For optical excitation in resonance with the E_1 band gap of InAs, both high- and low-frequency coupled longitudinal-optical phonon-intersubband plasmon modes are observed. From the measured energies of these plasmon modes the single-particle transition energies between the first and second confined electron subband were deduced as a function of the InAs well width. Good agreement was found with subband spacings predicted by theory including the effects of strain and nonparabolicity. InAs/AlSb surface quantum wells, where a pseudomorphically strained InAs quantum well is grown on an AlSb buffer layer without an AlSb top barrier, also show well-resolved intersubband plasmon modes, indicating higher-electron mobilities than those typically found in the surface inversion region of thick InAs layers.

There is considerable current interest in InAs/AlSb quantum-well (QW) structures, which offer the advantage of a low effective mass for electrons in the InAs QW ($m^*=0.023m_0$) in combination with a large conduction-band offset of 1.35 eV between the Γ -conduction-band minimum of InAs and the X -conduction-band minima of AlSb.¹ Such deep QW's for high mobility electrons are attractive for the fabrication of, e.g., high-speed quantum-well field-effect transistors.² InAs/AlSb QW's, in combination with superconducting Nb electrodes, have also recently made possible investigations of electronic interactions at superconductor-semiconductor interfaces.³ Due to the small fundamental band gap of InAs and the large conduction-band offset, which result in quantization energies for electrons comparable to the InAs band-gap energy for sufficiently narrow QW's, the nonparabolicity of the conduction band plays an important role in the description of the electronic properties of InAs/AlSb QW's.⁴ In the present paper we report on a systematic Raman spectroscopic study of intersubband transitions in InAs/AlSb QW's with various well widths. From the Raman data we are able to deduce the subband spacings, and these are found to be in good agreement with theoretical predictions taking full account of conduction-band nonparabolicities. Furthermore, intersubband Raman scattering was also observed from InAs/AlSb single heterostructures, in which the InAs QW is located at the sample surface.

Optical spectroscopy of intersubband transitions in QW's is a powerful technique to study the electron subband structure in general, and the effect of band nonparabolicity on the subband energies in particular. There is one report on IR intersubband spectroscopy on InAs/AlSb QW's.⁵ Inelastic light scattering by electronic intersubband excitations has found widespread use for the study of, e.g., GaAs/(AlGa)As quantum systems.⁶

For this material combination the fundamental band gap E_0 and the $E_0 + \Delta_0$ band gap are accessible by resonant Raman scattering. As these gaps involve the Γ -conduction-band minimum, where the electrons are located, inelastic light scattering by both collective charge-density and spin-density excitations^{6,7} as well as by single-particle intersubband transitions⁸ can be observed.

For InAs QW's, however, only the E_1 and $E_1 + \Delta_1$ band gaps lie in the spectral range accessible in resonant Raman experiments.⁹ Thus only coupled longitudinal-optical (LO) phonon-intersubband plasmon excitations, which may couple to the light via the electro-optic, deformation-potential, and Fröhlich mechanisms, can be observed in Raman scattering from InAs QW's.⁷ In semimetallic InAs/GaSb QW's both low- and high-frequency coupled intersubband plasmon-phonon modes have been resolved for optical excitation in resonance with the E_1 gap of InAs.¹⁰ For semiconducting InAs/AlSb QW's, only the high-frequency coupled intersubband plasmon-phonon mode has been observed so far.¹¹

The samples used for the present study were grown by solid-source molecular-beam epitaxy (MBE) on (100) GaAs substrates at temperatures ranging from 450 to 500 °C. Molecular beams of Sb₂ and As₂ were used, the latter being supplied by a valved cracker effusion cell.¹² Nonintentionally doped AlSb/InAs/AlSb single QW's with well widths ranging from 7.5 to 20 nm were grown on a 1- μ m-thick AlSb buffer layer. The thickness of the AlSb top barrier was 10 nm. Each structure was capped with a 10-nm GaSb layer. The shutter sequence for the growth of the InAs/AlSb heterointerfaces was chosen, if not stated otherwise, such as to deposit 1 monolayer (ML) InSb, which promotes the formation of InSb-like interfaces.¹³ In addition, 15-nm-thick single InAs layers were also grown on top of an AlSb buffer layer. These single InAs layers, or surface QW's, were deposited with in-

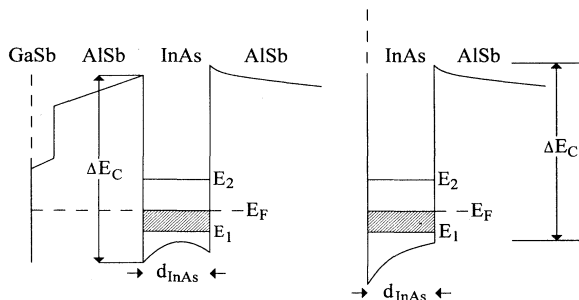


FIG. 1. Schematic conduction band profiles of an undoped GaSb-capped AlSb/InAs/AlSb single QW (left) and an InAs/AlSb surface QW (right).

terfacial layer sequences corresponding to the deposition of either 1-ML InSb or 1-ML AlAs.

Nonintentionally doped InAs/AlSb QW's have been found to contain electrons at concentrations ranging from a few times 10^{11} cm^{-2} to about $1 \times 10^{12} \text{ cm}^{-2}$, depending on details of the sample structure such as the top barrier thickness.¹⁴ Three sources of these electrons have been identified: deep donors in the nominally undoped AlSb barriers, InAs/AlSb interface donors, and donor states at the surface of the GaSb capping layer.¹⁴ For thicknesses of the AlSb top barrier below 50 nm, the contribution from the surface donors dominates.¹⁴ Conduction-band profiles of both the conventional AlSb/InAs/AlSb QW and the InAs/AlSb surface QW are shown schematically in Fig. 1. In the case of the surface QW, a large portion of the electrons present in the InAs QW originates from InAs surface states, which are known to lead to an *n*-type surface layer with the Fermi level at the surface pinned approximately 80 meV above the conduction-band edge.¹⁵

Raman measurements were carried out at room temperature with a spectral resolution of 2 cm^{-1} in back-

scattering from the (100) growth surface. Optical excitation was in the 2.54–2.6-eV range, close to the E_1 gap energy of InAs, to resonantly enhance scattering by coupled LO-phonon-intersubband plasmon modes.^{10,11}

In Fig. 2 Raman spectra of AlSb/InAs/AlSb QW's are plotted for various well widths. These spectra show for well widths $\geq 15 \text{ nm}$ the low-frequency coupled LO-phonon-intersubband plasmon mode ω_- at energies around 225 cm^{-1} , and the corresponding high-frequency coupled intersubband mode ω_+ in the energy range $1000\text{--}1400 \text{ cm}^{-1}$. The scattering strength decreases with decreasing well width, and for a width of 10 nm no intersubband mode is resolved. The longitudinal-optical (LO)-phonon signal observed slightly above the ω_- mode is a superposition of LO-phonon scattering in the InAs QW and in the GaSb capping layer because of the near coincidence of the LO mode frequencies in these two materials.¹¹

If the InAs conduction band is assumed to be parabolic, then the energies E_+ and E_- of the intersubband plasmon modes ω_+ and ω_- are given by^{6,7}

$$E_{\pm} = \frac{1}{2}(E_{12}^2 + E_{LO}^2 + E_P^2) \pm \frac{1}{2}[(E_{12}^2 + E_{LO}^2 + E_P^2) - 4(E_{12}^2 E_{LO}^2 + E_{TO}^2 E_P^2)]^{1/2}, \quad (1)$$

where E_{12} is the energy spacing between the first and second electron subbands, and E_P is the depolarization shift associated with the intersubband plasmon energy. For the present InAs/AlSb QW's we expect only the first subband to be filled,⁵ and thus the observed intersubband scattering signals to arise from scattering between the first and second subbands. E_{LO} and E_{TO} are the energies of the LO and transverse-optical (TO) phonons in the InAs quantum well, pseudomorphically strained to the in-plane lattice constant of the strain-relaxed AlSb buffer layer. These phonon energies ($E_{LO} = 232\text{--}233 \text{ cm}^{-1}$ and

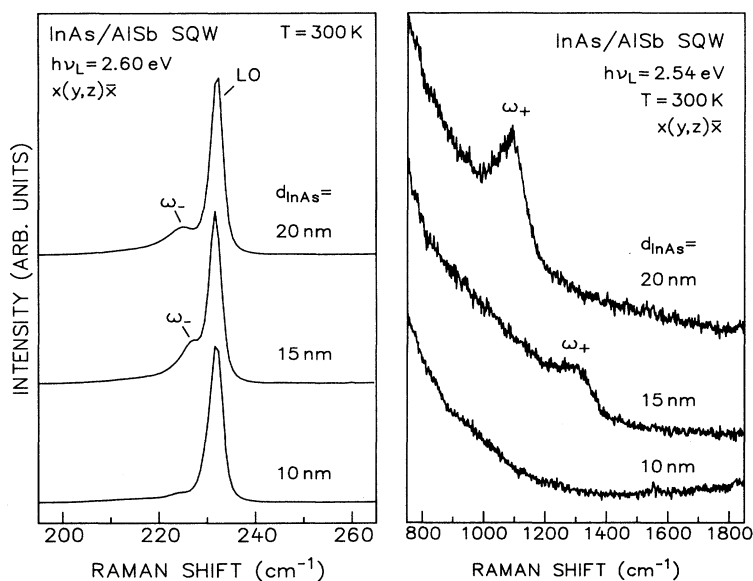


FIG. 2. Low-frequency (left) and high-frequency (right) portions of room-temperature Raman spectra from AlSb/InAs/AlSb single QW's of different widths d_{InAs} grown with InSb-like interfaces. The spectra were recorded with the polarizations of the scattered light perpendicular to that of the incident light $[x(y,z)\bar{x}]$, where x , y , and z denote [100], [010], and [001] crystallographic directions.

$E_{\text{TO}}=213\text{--}214\text{ cm}^{-1}$) were measured by Raman spectroscopy using in- and off-resonance excitation and various scattering polarization configurations.

Knowing E_+ , E_- , E_{LO} , and E_{TO} from the experiment, Eq. (1) can be solved for the subband spacing E_{12} and the depolarization shift E_P . The resulting subband spacing is plotted in Fig. 3 versus the width of the InAs QW (open circles). The data points for well widths of 15 and 20 nm were obtained from two pairs of samples grown at substrate temperatures of 450 and 500 °C, respectively, with 1-ML InSb deposited at each interface. The data point corresponding to a well width of 12.5 nm was taken from a QW sample grown at 500 °C, where 2-ML AlAs were deposited at the top interface. It has been shown that, at least for the present growth conditions, the addition of AlAs at the interface leads to segregation of As into the AlSb barriers,¹⁶ which in turn results in an enhanced two-dimensional (2D) electron concentration in the InAs QW.¹³ For comparison, subband spacings at the zone center ($k_{\parallel}=0$) for a square QW with finite barrier height, calculated employing a local energy-dependent effective mass,¹⁷ incorporating the effects of strain and nonparabolicity¹⁸ with band parameters for 300 K,¹⁹ are also shown in Fig. 3. These results agree to within 10 meV with those given in Ref. 20, obtained using low-temperature parameters. The effective masses for the first and second subbands, determined from the present calculations, were found to differ greatly due to nonparabolicity effects; e.g., for a 20-nm QW, E_{12} decreases by 19 meV from $k_{\parallel}=0$ to $k_{\parallel}=k_F \approx 2 \times 10^6\text{ cm}^{-1}$. Taking nonparabolicity and temperature into account in the calculation of the intersubband plasmon energies²¹ leads to an increase in E_{12} and E_P determined from a fit to the experimental results for E_+ and E_- , compared to values obtained using Eq. (1). Space-charge effects were not included, as they are expected to be small for the

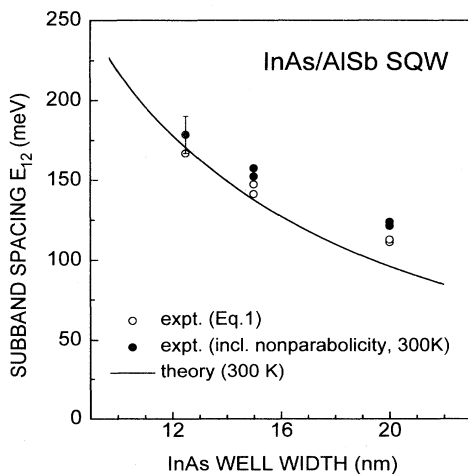


FIG. 3. Subband spacing E_{12} at $k_{\parallel}=0$ vs nominal InAs well width for AlSb/InAs/AlSb single QW's derived using Eq. (1) (open circles) and including nonparabolicity effects (filled circles). Error bars are indicated for the narrowest well width. Theoretical predictions taking into account the effect of strain and nonparabolicity are shown by the drawn curve.

present type of structure,²⁰ and the precise charge distribution under the present illumination conditions is not known. Resultant values for E_{12} ($k_{\parallel}=0$) are also shown in Fig. 3 (filled circles). The agreement between experiment and theory is good, given the approximations made in the theoretical determination of E_{12} . In addition, the present analysis is based on the nominal InAs QW widths based on growth rate calibrations. The actual thickness of the unperturbed binary InAs QW layer was found to be smaller by about 1.5 nm due to a finite thickness of the interface regions.²² Allowing for a similar reduction in the width of the electron confining potential well further improves the agreement between experiment and theory.

However, there is less agreement between the present Raman spectroscopic data and the IR-absorption data reported in Ref. 5. For nominally identical 15-nm-wide InAs/AlSb QW's, we find a subband spacing of 155 meV compared to a spacing of 95.4 meV given in Ref. 5. The energy of the ω_+ mode of 164 meV measured by Raman is significantly higher than the value of 113 meV found by IR absorption.⁵ This discrepancy could be resolved by applying both experimental techniques to the same set of QW samples.

The above-determined depolarization shift E_P is related to the 2D electron concentration N_{2D} by⁶ $E_P^2 = (2e^2/\epsilon\epsilon_0)L_{12}E_{12}N_{2D}$, where ϵ is the high-frequency dielectric constant of the QW material, ϵ_0 the vacuum permittivity, and L_{12} the Coulomb matrix element.⁶ With L_{12} calculated for a square QW with finite barrier height, the above expression can be solved for N_{2D} . For all the samples we obtain a 2D electron concentration in the range $5.5\text{--}7.0 \times 10^{11}\text{ cm}^{-2}$. Room-temperature Hall effect measurements on one of the 20-nm QW samples yield a 2D electron concentration of $1.7 \times 10^{12}\text{ cm}^{-2}$ as compared to the present Raman data, which give a concentration of $6.4 \times 10^{11}\text{ cm}^{-2}$. This difference can be explained by a negative photoeffect. Optical excitation with photon energies of $> 1.55\text{ eV}$ was found to lead to a drastic decrease in the 2D electron concentration.²³ Low-temperature transport measurements revealed a decrease to $\frac{1}{4}$ of the original value upon excitation with 2.25-eV photons.²³ Thus the present finding of a reduction in the room-temperature electron concentration upon intense illumination with 2.6–2.7-eV photons to about $\frac{1}{3}$ of the concentration measured in the dark is consistent with the results cited above.

Figure 4 shows Raman spectra of two 15-nm-wide InAs/AlSb surface QW's nominally grown with either an InSb-like or an AlAs-like interface. For comparison, the low-frequency portion of the Raman spectrum of a strain-relaxed and nominally undoped InAs layer grown heteroepitaxially on (100) GaAs is also shown. The surface quantum wells show well-resolved low- and high-frequency intersubband plasmon-phonon modes along with scattering by the InAs LO phonon. The energies and widths of these plasmon modes indicate a higher 2D electron concentration and lower electron mobility for the surface QW with a nominally AlAs-like interface than for that with an InSb-like interface. This finding is in agreement with transport data obtained for conventional AlSb/InAs/AlSb QW's.¹³ The Raman spectrum of

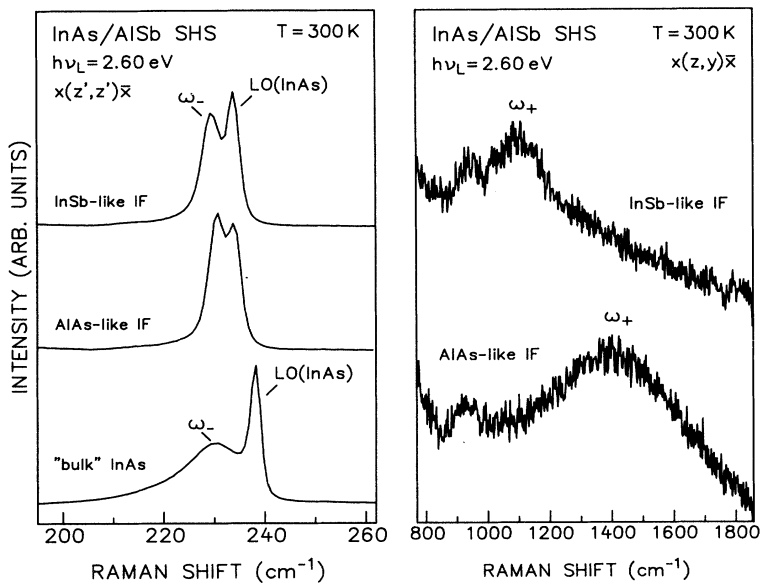


FIG. 4. Low-frequency (left) and high-frequency (right) portions of room-temperature Raman spectra from pseudomorphic InAs/AlSb surface QW's grown with either an InSb-like or an AlAs-like interface (IF). For comparison, the low-frequency portion of the Raman spectrum of a nominally undoped bulklike InAs layer is also shown. The spectra were recorded with the polarizations of the incident and scattered light either parallel to the same [110] crystallographic direction $[x(z',z')\bar{x}]$ (left) or perpendicular to each other $[x(z,y)\bar{x}]$, where x , y , z , and z' denote [100], [010], [001], and [011] crystallographic directions.

the n -type surface inversion layer in bulklike InAs,²⁴ in contrast, shows only a broadened low-frequency plasmon peak and no detectable scattering from a high-frequency mode. This observation indicates that the mobility of the 2D electron gas in an InAs/AlSb surface QW is improved over that found in a n -type inversion layer.

In conclusion, we studied intersubband excitations in InAs/AlSb QW's by resonant Raman scattering. For conventional AlSb/InAs/AlSb QW's the spacing between the first and second electrons subbands was determined as a function of the well width. Good agreement was found with theoretical predictions including nonparabolicities. InAs/AlSb surface QW's were found to show well-

resolved scattering peaks due to low- and high-frequency intersubband plasmon-phonon modes, in contrast to the n -type surface inversion layer in a bulklike InAs reference sample.

We would like to thank G. Bihlmann for valuable technical assistance in the MBE growth, F. Pohl for technical support of the Raman experiments, and P. Hiesinger for performing the Hall-effect measurements. The Bundesministerium für Forschung und Technologie is thanked for financial support within the program "III-V Electronics."

¹A. Nakagawa, H. Kroemer, and J. H. English, *Appl. Phys. Lett.* **54**, 1893 (1989).

²G. Tuttle and H. Kroemer, *IEEE Trans. Electron. Dev.* **ED-34**, 2358 (1987).

³C. Nguyen, H. Kroemer, and E. L. Hu, *Phys. Rev. Lett.* **69**, 2847 (1992).

⁴M. J. Yang, P. J. Lin-Chung, B. V. Shanabrook, J. R. Waterman, R. J. Wagner, and W. J. Moore, *Phys. Rev. B* **47**, 1691 (1993).

⁵A. Simon, J. Scriba, C. Gauer, A. Wixforth, J. P. Kotthaus, C. R. Bolognesi, C. Nguyen, G. Tuttle, and H. Kroemer, *Mater. Sci. Eng. B* **21**, 201 (1993).

⁶See, e.g., A. Pinczuk and G. Abstreiter, in *Light Scattering in Solids V*, edited by M. Cardona and G. Güntherodt (Springer, Berlin, 1989), p. 153.

⁷E. Burstein, A. Pinczuk, and D. L. Mills, *Surf. Sci.* **98**, 451 (1980).

⁸A. Pinczuk, S. Schmitt-Rink, G. Danan, J. P. Valladares, L. N. Pfeiffer, and K. W. West, *Phys. Rev. Lett.* **63**, 1633 (1989).

⁹R. Carles, N. Saint-Cricq, J. B. Renucci, M. A. Renucci, and A. Zwick, *Phys. Rev. B* **22**, 4804 (1980).

¹⁰Y. B. Li, V. Tsoukala, R. A. Stradling, R. L. Williams, S. J. Chung, I. Kamiya, and A. G. Norman, *Semicond. Sci. Technol.* **8**, 2205 (1993).

¹¹J. Wagner, J. Schmitz, J. D. Ralston, and P. Koidl, *Appl. Phys. Lett.* **64**, 82 (1994).

¹²J. Schmitz, J. Wagner, M. Maier, H. Obloh, P. Koidl, and J. D. Ralston, *J. Electron. Mater.* **23**, 1203 (1994).

¹³G. Tuttle, H. Kroemer, and J. H. English, *J. Appl. Phys.* **67**, 3032 (1990).

¹⁴C. Nguyen, B. Brar, H. Kroemer, and J. H. English, *Appl. Phys. Lett.* **60**, 1854 (1992).

¹⁵See, e.g., Ch. Nguyen, B. Brar, and H. Kroemer, *J. Vac. Sci. Technol. B* **11**, 1706 (1993).

¹⁶J. Wagner, J. Schmitz, D. Behr, J. D. Ralston, and P. Koidl, *Appl. Phys. Lett.* **65**, 1293 (1994).

¹⁷R. Lassnig, *Phys. Rev. B* **31**, 8076 (1985).

¹⁸G. Hendorfer and J. Schneider, *Semicond. Sci. Technol.* **6**, 595 (1991).

¹⁹*Semiconductors. Physics of Group IV Elements and III-V Compounds*, edited by O. Madelung, Landolt-Börnstein, New Series, Group III, Vol. 17, Pt. a (Springer, Heidelberg, 1982).

- ²⁰P. J. Lin-Chung and M. J. Yang, *Phys. Rev. B* **48**, 5338 (1993).
²¹G. Brozak, B. V. Shanabrook, D. Gammon, D. A. Broido, R. Beresford, and W. I. Wang, *Phys. Rev. B* **45**, 11 399 (1992).
²²F. Fuchs, J. Schmitz, K. Schwarz, J. Wagner, J. D. Ralston, P. Koidl, C. Gadaleta, and G. Scamarcio, *Appl. Phys. Lett.* **65**, 2060 (1994).

- ²³Ch. Gauer, J. Scriba, A. Wixforth, J. P. Kotthaus, C. Nguyen, G. Tuttle, J. H. English, and H. Kroemer, *Semicond. Sci. Technol.* **8**, S137 (1993).
²⁴L. Y. Ching, E. Burstein, S. Buchner, and H. H. Wieder, *J. Phys. Soc. Jpn. A* **49**, 951 (1980).